

Non-adiabatic dynamics across a first order quantum phase transition: Quantized bubble nucleation

Aritra Sinha,^{1,*} Titas Chanda,^{1,†} and Jacek Dziarmaga^{1,‡}

¹*Institute of Theoretical Physics, Jagiellonian University, Łojasiewicza 11, 30-348 Kraków, Poland*

(Dated: June 10, 2021)

Metastability is a quintessential feature of first order quantum phase transitions, which is lost either by dynamical instability or by nucleating bubbles of a true vacuum through quantum tunneling. By considering a drive across the first order quantum phase transition in the quantum Ising chain in the presence of both transverse and longitudinal fields, we reveal multiple regions in the parameter space where the initial metastable state loses its metastability in successive stages. The mechanism responsible is found to be semi-degenerate resonant tunnelings to states with specific bubble sizes. We show that such dynamics of *quantized* bubble nucleations can be understood in terms of Landau-Zener transitions, which provide quantitative predictions of nucleation probabilities for different bubble sizes.

Introduction.— Non-equilibrium aspects of many-body quantum systems are at the heart of understanding the fundamentals of statistical and condensed matter physics as well as of quantum field theory [1–9]. On the theoretical front, the analysis of the dynamics of non-integrable systems have soared drastically during the last two decades due to the advancement and development of efficient numerical tools like various tensor networks methods [10–12]. Moreover, with the recent breakthroughs in quantum simulations [13–19], studying the non-equilibrium features of complex quantum systems on table-top experiments has become a reality, especially in the substrates like cold-atoms on optical lattices [20–25] or trapped ions [26–33].

One promising avenue of work in this ubiquitous facet of fundamental physics has been to investigate non-adiabatic excitations due to quenches across a continuous quantum phase transition [34, 35] under the unifying framework of the quantum version [6, 36–40] of the classic Kibble-Zurek (KZ) mechanism [41–46]. However, the question that has been asked less frequently is regarding the consequence of a slow drive across a first order quantum phase transition (FOQPT) [47, 48] and whether it is possible to find any similar universal dynamical features akin to quantum KZ theory.

FOQPTs exhibit metastability on a drive across the transition, i.e., the system tends to persist in the local minimum due to the presence of a potential barrier. In the traditional language of continuous field theory, the state gets stuck in a false vacuum, that is stable against small fluctuations, and cannot tunnel to the true vacuum easily. However, on a dynamical quench across FOQPT, the false vacuum may become dynamically unstable and the true vacuum may develop due to the disappearance of the potential barrier far beyond the FOQPT point. Under such scenarios, several recent studies reported KZ scaling laws for the dynamics across certain first order phase transitions – both classical as well as quantum [49–57]. Another more generic mechanism, through which such metastability can evaporate, is the continual

creation of bubbles of the true vacuum driven by the quantum fluctuations inside the false vacuum. The aim of the present letter is to thoroughly investigate breakdown of metastability by the nucleation of bubbles in a many-body quantum setting – going beyond the paradigm of dynamical instability and the corresponding KZ mechanism.

We consider the generic one-dimensional (1D) quantum Ising chain in the presence of both transverse and longitudinal fields. The model possesses a FOQPT between two ferromagnetic phases of opposite orientations driven by the longitudinal field. On slow tuning of the longitudinal field across the FOQPT line, we detect a multitude of special (resonant) points/regions where the nucleation of bubbles of the true vacuum inside the metastable false vacuum becomes energetically favorable. Moreover, these tunneling processes are *quantized* in the sense that only a specific size of bubbles, pertaining to a specific perturbative order, can nucleate around the corresponding resonant value of the longitudinal field. We provide accurate quantitative explanations of these non-adiabatic changes by means of the archetypal Landau-Zener (LZ) theory [58–61].

Model.— The quantum Ising model in the presence of a transverse field in 1D is one of the prototypical models used for several decades to understand the quantum phase transition at zero temperature [34, 35]. In the presence of an additional longitudinal field the Hamiltonian reads

$$H = - \sum_{n=1}^N [\sigma_n^z \sigma_{n+1}^z + h_x \sigma_n^x + h_z \sigma_n^z], \quad (1)$$

where we assume transverse field $h_x > 0$ for definiteness. Apart from having a rich phase diagram, this model, although being simple, has become a test-bed for fascinating equilibrium as well as out-of-equilibrium phenomena, like weak-thermalization [62], dynamical confinement [63–66], existence of quantum many-body scars [67–69], or fracton dynamics [70]. For the

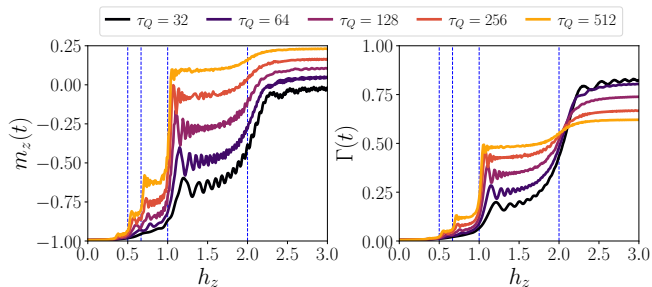


FIG. 1. The average magnetization $m_z(t)$ (left) and the density of kinks $\Gamma(t)$ (right) tracked dynamically by varying the parallel field h_z according to Eq. (2) for a wide range of quench times τ_Q . Here we set $h_x = 0.2$ and $h_z^{\text{in}} = -4.0$.

longitudinal field $h_z = 0$, this model has a continuous quantum phase transition at $h_x = 1$ separating the ferromagnetic phase ($h_x < 1$) from the paramagnetic one ($h_x > 1$). An FOQPT exists separating two ordered ferromagnetic phases along the so-called Ising line ($h_z = 0$). In this letter, we will mostly stay in the regime of small transverse field, $h_x \ll 1$ (although this is not a strict requirement), where, with the exception of some special regions, it can be considered as a source of small quantum fluctuations in a classical Ising chain.

Linear ramp and special regions.— To initiate, we prepare the system in the ground state of the Hamiltonian (1) in one of the ordered phases ($h_x < 1$) and perform a slow ramp of the longitudinal field h_z across the first order transition. We choose a protocol akin to what is usually used in studies of the KZ mechanism, where we ramp the field as

$$h_z(t) = h_z^{\text{in}} + \frac{t}{\tau_Q}. \quad (2)$$

We start at time $t = 0$ when the initial state $|\psi(t=0)\rangle = |\psi_{\text{in}}\rangle$ is the ground state of the Hamiltonian (1) with $h_z^{\text{in}} < 0$, and then ramp the field up to a final value $h_z^{\text{fin}} > 0$ in the opposite ordered phase. The total ramp time is proportional to τ_Q . The dynamics is simulated by using time-dependent variational principle (TDVP) [12, 71–73] based on matrix-product state (MPS) [10, 11] ansatz with open boundary condition.

To start, we use average longitudinal magnetization $m_z = \frac{1}{N} \sum_n \langle \sigma_n^z \rangle$, and the longitudinal density of kinks $\Gamma = \frac{1}{2} \left(1 - \frac{1}{N-1} \sum_n \langle \sigma_n^z \sigma_{n+1}^z \rangle \right)$ as our *bona fide* observables. Deep in the ferromagnetic phase, for $|h_z^{\text{in}}| \gg h_x$, the initial state has $m_z \approx -1$ and $\Gamma \approx 0$ as the state is highly polarized:

$$|\psi_{\text{in}}\rangle \approx |\downarrow \downarrow \dots \downarrow\rangle. \quad (3)$$

During the ramp, we observe that the initial state remains metastable against small quantum fluctuations driven by the transverse h_x for a long time after crossing

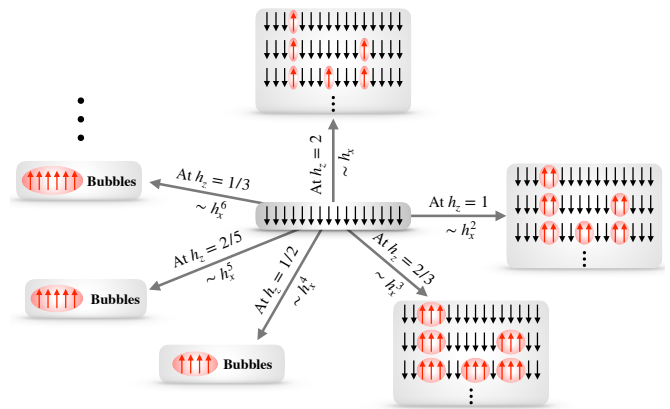


FIG. 2. Diagram showing the possible nucleation processes and their perturbative orders in h_x . At $h_z = 2/n$ the metastable initial state, with all spins pointing down, is semi-degenerate with states containing size- n bubbles with spins up. They are connected by an n -th order process in h_x .

the FOQPT point. The crucial feature in this scenario is that the system departs from the metastable state at several *special occasions* during the ramp, see Fig. 1. Deep into the positive ferromagnetic phase ($h_z > 0$), the average magnetization $m(t)$ and the density of kinks $\Gamma(t)$ get jolted up in several steps and finally saturates although with visible small oscillations. We shall show that these special regions exist around points where the initial metastable state is semi-degenerate with bubbles of the true vacuum. Below, we provide an heuristic explanation first.

Without quantum fluctuations, when the knob is set to $h_x = 0$, any spin flips in the fully polarized initial state (3) increases the ferromagnetic energy – a domain or bubble of n consecutive \uparrow -spins increases the ferromagnetic energy by 4, regardless of its size. Overall, taking into account the local longitudinal fields, such a bubble of size n changes the total energy by $4 - 2nh_z$, which becomes zero when

$$h_z = 2/n. \quad (4)$$

As a result, we have *quantized* values of the longitudinal field $h_z = 2, 1, 2/3, 1/2, \dots$, where the initial metastable state becomes degenerate with states having bubbles of sizes $n = 1, 2, 3, 4, \dots$, respectively. These are the four major quantized values of the longitudinal magnetic field that correspond to the jolts clearly seen in Fig. 1.

When $h_x > 0$, operators σ_n^z are no longer good quantum numbers. For a generic h_z , the initial state (3), dressed with quantum fluctuations of second order in h_x , remains an approximate eigenstate. This is not the case at the special quantized values of h_z , where the initial state becomes semi-degenerate with bubbles of size n – connected by anticrossings – and even a tiny h_x is enough to mix them. Each of these *resonant points* in h_z corresponds to a particular order in perturbation

theory with respect to h_x . For instance, only nucleations of bubble-size 1 can happen near $h_z = 2$. As this requires a single spin to be flipped, the tunneling between the degenerate states is first order in h_x . In general, tunneling at $h_z = 2/n$ between the polarized initial state and a state with an n -bubble is an n -th order process. For a schematic viewpoint see Fig. 2.

Landau-Zener (LZ) nucleation theory.— We begin with $n = 1$ near $h_z = 2$. For low density of flipped spins, we can consider flipping an isolated spin at site j :

$$|\downarrow \dots \downarrow \downarrow_j \downarrow \dots \downarrow\rangle \xleftrightarrow{h_x} |\downarrow \dots \downarrow \uparrow_j \downarrow \dots \downarrow\rangle. \quad (5)$$

The tunneling is driven by the term $-h_x \sigma_j^x$. In the two dimensional subspace, the Hamiltonian reads

$$H_{\text{eff}}^{(1)} = E_0(h_z) + \begin{bmatrix} 0 & -h_x \\ -h_x & 4 - 2h_z \end{bmatrix}, \quad (6)$$

where $E_0(h_z) = -(N - 1) + Nh_z$ is the energy of the metastable state. With the linear ramp (2) this becomes the LZ problem [58–61] with an anticrossing when $h_z = 2$. The LZ probability to flip the spin is $p_1 = 1 - \exp(-\pi \tau_Q h_x^2)$. Beyond the two-dimensional subspace, this formula is accurate only when $p_1 \ll 1$ or, equivalently, for fast quenches with $\pi \tau_Q h_x^2 \ll 1$. Otherwise, the density of flipped spins becomes large and we cannot consider flipping spin j in isolation from flipping other spins.

More generally, bubbles of n spins are nucleated near $h_z = 2/n$. For a low total density of bubbles we can consider flipping n consecutive spins $j, \dots, j + n - 1$ by a n -th order process:

$$|\downarrow \dots \downarrow \downarrow_j \dots \downarrow_{j+n-1} \downarrow \dots \downarrow\rangle \xleftrightarrow{h_x^n} |\downarrow \dots \downarrow \uparrow_j \dots \uparrow_{j+n-1} \downarrow \dots \downarrow\rangle. \quad (7)$$

For such a process the effective Hamiltonian reads

$$H_{\text{eff}}^{(n)} \approx E_0(h_z) + \begin{bmatrix} 0 & -c_n h_x^n \\ -c_n h_x^n & 4 - 2n h_z \end{bmatrix}. \quad (8)$$

Here c_n is a combinatorial factor. In general, it can be derived for any order n by treating the transverse field perturbatively and obtaining the low-energy effective Hamiltonian through the Schrieffer-Wolff transformation [74]. For particular perturbative orders, we will concentrate on $c_1 = c_2 = 1$ and $c_3 = 81/64$ in this letter [75]. After the anticrossing at $h_z \approx 2/n$ the LZ probability to nucleate the n -bubble reads [75]

$$p_n = 1 - \exp\left(-\frac{c_n^2}{n} \pi \tau_Q h_x^{2n}\right) \approx \frac{c_n^2}{n} \pi \tau_Q h_x^{2n}. \quad (9)$$

It is accurate for $\tau_Q h_x^{2n} \ll 1$ only. In order to verify the LZ formula, we consider the density of n -bubbles:

$$\lambda_n = \left\langle P_i^\downarrow \left[\prod_{j=1}^n P_{i+j}^\uparrow \right] P_{i+n+1}^\downarrow \right\rangle. \quad (10)$$

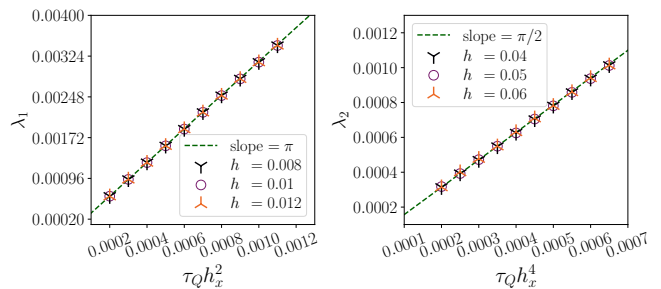


FIG. 3. The density of 1-bubbles, λ_1 (left), and 2-bubbles, λ_2 (right), are shown as functions of scaled τ_Q for several strengths h_x of quantum fluctuations. The different h_x collapse to straight lines with slopes π and $\pi/2$ for $n = 1, 2$, respectively. The collapse demonstrates the accuracy of the simple Landau-Zener theory for low density of nucleated bubbles.

Here $P_j^{\uparrow, \downarrow} = (1 \pm \sigma_j^z)/2$ is a projector onto spin- \uparrow (\downarrow) at site j and $\langle \dots \rangle$ refers to averaging over all sites except for the ends of the chain to avoid boundary effects. In Fig. 3 we plot λ_1 and λ_2 obtained with TDVP as a function of $\tau_Q h_x^{2n}$ for several values of h_x such that the low density condition, $\tau_Q h_x^{2n} \ll 1$, is satisfied. Plots for different h_x collapse to a straight line with a slope consistent with the simple LZ theory.

Nucleation versus hopping.— In the second order perturbation in h_x , the n -bubble at sites $j, \dots, j + n - 1$ can hop to the right/left by one lattice site. In order to hop to the right, spin $j + n$ can be flipped upwards followed by a downward flip of spin j , or the other way round. The net hopping rate is $\gamma = h_x^2/h_z$.

The LZ formula cannot be taken for granted if the nucleated bubble can hop away before the LZ tunneling is completed at time $t_{\text{LZ}} \approx \sqrt{\tau_Q/2n}$ [36] after the anticrossing at $h_z = 2/n$. Therefore, the hopping should be irrelevant when $\gamma t_{\text{LZ}} \ll 1$ or, equivalently,

$$\frac{1}{8} n \tau_Q h_x^4 \ll 1. \quad (11)$$

For 1-bubbles this condition is satisfied with a safe margin in their low density regime where $\pi \tau_Q h_x^2 \ll 1$. For 2-bubbles it is identical with low density. However, for 3-bubbles and bigger it is stronger than low density. For 3-bubbles the hopping is a second order process while the LZ tunneling is formally a weaker third order effect.

In order to demonstrate the interplay between the nucleation of 3-bubbles and their hopping we simulate a ramp from $h_z^{\text{in}} = -6$ to $h_z^{\text{fin}} = 0.8$. The density of 3-bubbles is shown in Fig. 4 as a function of the scaling variable deep in the low density regime, where $\tau_Q h_x^6 \ll 1$. With increasing $\tau_Q h_x^6$ there is a crossover from the pure LZ nucleation to the regime where the hopping becomes relevant. In the former we can see good agreement with the LZ theory, demonstrated by the collapse, while in the latter the curves begin to diverge slowly.

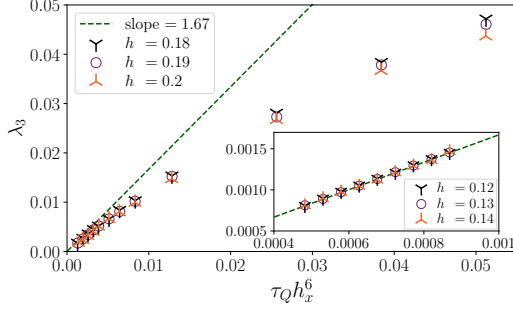


FIG. 4. Density of 3-bubbles, λ_3 , as a function of the scaling variable $\tau_Q h_x^6$ for different values of h_x . Here $\tau_Q h_x^6 \ll 1$ is deep in the low density regime but, according to condition (11), the hopping remains irrelevant at most up to $\tau_Q h_x^6 \approx h_x^2 \approx 0.03$. To the left of this point the plots collapse to a single curve that tends to a line with the predicted slope $\frac{1}{3}(81/64)^2\pi = 1.67$ (see the inset). To the right the plots begin to diverge demonstrating the breakdown of the simple LZ theory.

Beyond low density.— Upto now, we have seen that bubble nucleations at low densities are accurately described by two-level LZ problems. Moreover, for $n = 1, 2, 3$, $\tau_Q h_x^{2n}$ is the scaling variable when the hopping is not relevant. The next natural questions are (1) if it remains such beyond the low density regime, and (2) whether we can also treat bubble nucleations at high densities as LZ transitions. To answer these questions, we consider again the nucleation of 1-bubbles near $h_z = 2$ but this time in full range of $\tau_Q h_x^2$. In order to isolate the 1-bubble nucleation in full TDVP simulations, we have to keep irrelevant not only the hopping (11) but also the 3- and 2-bubble nucleation at $h_z = 2/3, 1$, respectively. This requires very small h_x^2 that makes τ_Q rather long, making TDVP intractable for $\tau_Q h_x^2 \gg 1$.

In order to get perfect isolation and additionally get some analytical insights, first we consider an effective Hamiltonian by projecting the original Hamiltonian (1) into the 1-bubble subspace. On a periodic chain of N sites the subspace is spanned by the initial metastable state $|0\rangle = |\psi_{\text{in}}\rangle$ in (3), the translationally invariant (TI) one 1-bubble state, $|1\rangle = \frac{1}{\sqrt{N}} \sum_j |\downarrow \dots \downarrow \uparrow_j \downarrow \dots \downarrow\rangle$, TI two 1-bubble state $|2\rangle$, upto the TI state with $N/2$ 1-bubbles $|N/2\rangle = \frac{1}{\sqrt{2}}(|\downarrow \uparrow \downarrow \uparrow \dots\rangle + |\uparrow \downarrow \uparrow \downarrow \dots\rangle)$. It turns out that the resulting $(N/2 + 1)$ -dimensional effective Hamiltonian can be constructed iteratively, see [75], and for our purpose we can consider up to $N = 44$ using a standard 64-bit machine.

Similarly as (6), the resulting Hamiltonian is a linear combination of two terms [75]:

$$H_{\text{eff}} = \tilde{E}_0 + \frac{t}{\tau_Q} H_z + h_x H_x, \quad (12)$$

with $\tilde{E}_0 = \langle 0|H(h_z = 2, h_x = 0)|0\rangle$. This structure allows us to rewrite the Schrödinger equation, $i \frac{d|\psi\rangle}{dt} =$

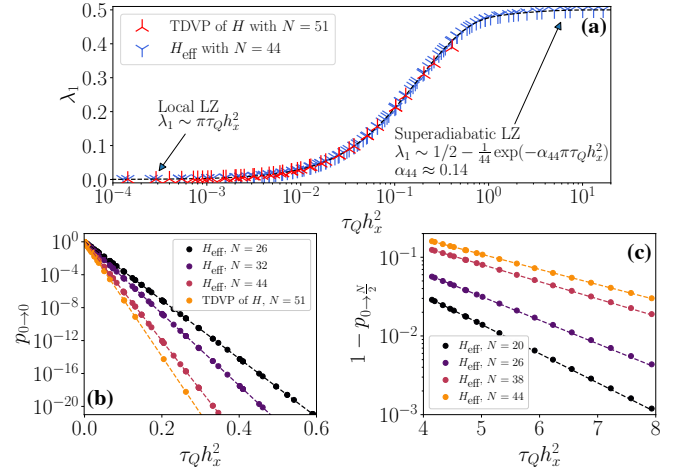


FIG. 5. (a) Density of 1-bubbles λ_1 as a function of $\tau_Q h_x^2$ after a ramp across $h_z = 2$. Here the effective Hamiltonian (12) is benchmarked against direct TDVP simulation. The curve crosses over from the low density linearized LZ formula (9) with $n = 1$ to the high density LZ profile (16). (b) The multi-level LZ transition probability $p_{0 \rightarrow 0}$ as a function of $\tau_Q h_x^2$ for different system sizes N . The dashed line is the analytical formula: $p_{0 \rightarrow 0} = \exp[-N\pi\tau_Q h_x^2]$. (c) The superadiabatic transition probability $p_{0 \rightarrow \frac{N}{2}}$ as a function of $\tau_Q h_x^2$ for different N fitted with the exponential function $p_{0 \rightarrow \frac{N}{2}} = 1 - \exp[-\alpha_N \pi \tau_Q h_x^2]$.

$H_{\text{eff}}|\psi\rangle$, as $i \frac{d}{dt'} |\psi'\rangle = \left(\frac{t'}{\tau_Q h_x^2} H_z + H_x \right) |\psi'\rangle$. Here $t' = h_x t$ and \tilde{E}_0 was absorbed in the phase of $|\psi'\rangle$. This demonstrates that the final density of 1-bubbles must depend on $\tau_Q h_x^2$ as a single scaling variable.

The dependence, obtained by simulation with the effective Hamiltonian, is plotted in Fig. 5(a). The same figure compares results from full TDVP simulations. Unlike the low density regime, the generic problem now is that of a $(N/2 + 1)$ -level LZ transition, which again in the low density regime reduces to the local two level LZ scenario. To describe such a multi-level LZ problem, we consider two transition probabilities:

$$\begin{aligned} p_{0 \rightarrow 0} &= \lim_{t \rightarrow \infty} |\langle 0|\psi(t)\rangle|^2, \\ p_{0 \rightarrow \frac{N}{2}} &= \lim_{t \rightarrow \infty} |\langle N/2|\psi(t)\rangle|^2. \end{aligned} \quad (13)$$

Following Ref. [76], the former one has the exact form:

$$p_{0 \rightarrow 0} = \exp \left[-2\pi\tau_Q h_x^2 \sum_{n=1}^{N/2} \frac{|\langle n|H_x|0\rangle|^2}{|\langle n|H_z|n\rangle - \langle 0|H_z|0\rangle|} \right], \quad (14)$$

which translates into $p_{0 \rightarrow 0} = \exp[-N\pi\tau_Q h_x^2]$ [75]. Fig. 5(b) shows the profile of $p_{0 \rightarrow 0}$ for different values of N that perfectly matches the analytical prediction. Moreover, for $\tau_Q h_x^2 \ll 1$ only transitions between $|0\rangle$ and states $|n\rangle$ with low density, $n \ll N$, become relevant. The total probability of these transitions is $1 - p_{0 \rightarrow 0}$.

Therefore, in this regime the density of 1-bubbles $\lambda_1 = \frac{1}{N}(1 - p_{0 \rightarrow 0}) \approx \pi\tau_Q h_x^2$ confirming the earlier analysis again.

On the other hand, when the curve in Fig. 5(a) reaches the superadiabatic regime, $\tau_Q h_x^2 \gg 1$, there is only one relevant LZ anticrossing. The initial metastable state $|0\rangle$ crosses over to the final state $|N/2\rangle$ with probability $p_{0 \rightarrow \frac{N}{2}}$ and $(1 - p_{0 \rightarrow \frac{N}{2}})$ becomes a small excitation probability to the state $|N/2 - 1\rangle$. An analytical derivation of $p_{0 \rightarrow \frac{N}{2}}$ from the multi-level LZ problem is beyond the scope this work. However, we find the following form

$$p_{0 \rightarrow \frac{N}{2}} = 1 - \exp[-\alpha_N \pi \tau_Q h_x^2], \quad (15)$$

where the coefficient α_N decreases with N [75], see Fig. 5(c). Therefore, the 1-bubble density in this regime is

$$\begin{aligned} \lambda_1 &= \frac{1}{N} \left[\frac{N}{2} p_{0 \rightarrow \frac{N}{2}} + \left(\frac{N}{2} - 1 \right) (1 - p_{0 \rightarrow \frac{N}{2}}) \right] \\ &= \frac{1}{2} - \frac{1}{N} (1 - p_{0 \rightarrow \frac{N}{2}}), \end{aligned} \quad (16)$$

which is in good agreement with Fig. 5(a).

Conclusion and outlook.— We have shown that the metastability pertained to FOQPT in the quantum Ising model under transverse and longitudinal fields is lost in successive stages in quenches across the FOQPT point, that occurs due to *quantized* the nucleation of bubbles. Specifically, we have identified special resonant regions in the longitudinal field ($h_z = 2/n$), where the metastable state can easily tunnel to nucleate bubbles of specific size n , which are n -th order perturbative processes in the transverse field h_x . Moreover, we have unified this entire non-adiabatic process under the umbrella of Landau-Zener theories – the low density nucleations can be understood through two-level Landau-Zener transitions, while at higher densities the situations translate to the multi-level Landau-Zener problems.

Furthermore, our work can be easily generalized to higher dimensions, where the special resonant points become $h_z \propto S/V$. Here S is the surface area and V the volume of a bubble, each of them taking discrete values. The physical implementation of the transverse Ising model with a chain of Rydberg atoms provided spectacular demonstration [25] of the quantum Kibble-Zurek mechanism. Within two years following this breakthrough, the number of Rydberg atoms increased from 50 in 1D [25] to a few hundred in 2D/3D structures [77, 78]. Such marvelous achievements on the experimental front make possible to explore regimes where the nucleation of bubbles manifests a quantized nature, not only in 1D but also in higher dimensions.

We are grateful to Marek M. Rams, Debasis Sadhukhan, Jakub Zakrzewski, Maciej Lewenstein, and Luca Tagliacozzo for useful discussions and valuable comments. We acknowledge funding by

the National Science Centre (NCN), Poland together with European Union through QuantERA ERA NET programs: NAQUAS 2017/25/Z/ST2/03028 (AS, JD) and QTFLAG 2017/25/Z/ST2/03029 (TC).

* aritrasinha98@gmail.com

† titas.chanda@uj.edu.pl

‡ dziarmaga@th.if.uj.edu.pl

- [1] M. Srednicki, Chaos and quantum thermalization, *Phys. Rev. E* **50**, 888 (1994).
- [2] P. Calabrese and J. Cardy, Entanglement entropy and quantum field theory, *Journal of Statistical Mechanics: Theory and Experiment* **2004**, P06002 (2004).
- [3] P. Calabrese and J. Cardy, Evolution of entanglement entropy in one-dimensional systems, *Journal of Statistical Mechanics: Theory and Experiment* **2005**, P04010 (2005).
- [4] M. Rigol, V. Dunjko, and M. Olshanii, Thermalization and its mechanism for generic isolated quantum systems, *Nature* **452**, 854 (2008).
- [5] P. Calabrese and J. Cardy, Entanglement entropy and conformal field theory, *Journal of Physics A: Mathematical and Theoretical* **42**, 504005 (2009).
- [6] A. Polkovnikov, K. Sengupta, A. Silva, and M. Vengalattore, Colloquium: Nonequilibrium dynamics of closed interacting quantum systems, *Rev. Mod. Phys.* **83**, 863 (2011).
- [7] J. Eisert, M. Friesdorf, and C. Gogolin, Quantum many-body systems out of equilibrium, *Nature Physics* **11**, 124 (2015).
- [8] L. D'Alessio, Y. Kafri, A. Polkovnikov, and M. Rigol, From quantum chaos and eigenstate thermalization to statistical mechanics and thermodynamics, *Advances in Physics* **65**, 239 (2016).
- [9] D. Rossini and E. Vicari, Coherent and dissipative dynamics at quantum phase transitions (2021), [arXiv:2103.02626 \[cond-mat.stat-mech\]](https://arxiv.org/abs/2103.02626).
- [10] U. Schollwöck, The density-matrix renormalization group in the age of matrix product states, *Annals of Physics* **326**, 96 (2011).
- [11] R. Orús, A practical introduction to tensor networks: Matrix product states and projected entangled pair states, *Annals of Physics* **349**, 117 (2014).
- [12] S. Paeckel, T. Köhler, A. Swoboda, S. R. Manmana, U. Schollwöck, and C. Hubig, Time-evolution methods for matrix-product states, *Annals of Physics* **411**, 167998 (2019).
- [13] R. P. Feynman, Simulating physics with computers, *International Journal of Theoretical Physics* **21**, 467 (1982).
- [14] T. H. Johnson, S. R. Clark, and D. Jaksch, What is a quantum simulator?, *EPJ Quantum Technology* **1**, 10 (2014).
- [15] J. I. Cirac and P. Zoller, Goals and opportunities in quantum simulation, *Nature Physics* **8**, 264 (2012).
- [16] I. Bloch, J. Dalibard, and S. Nascimbène, Quantum simulations with ultracold quantum gases, *Nature Physics* **8**, 267 (2012).
- [17] R. Blatt and C. F. Roos, Quantum simulations with trapped ions, *Nature Physics* **8**, 277 (2012).

- [18] A. Aspuru-Guzik and P. Walther, Photonic quantum simulators, *Nature Physics* **8**, 285 (2012).
- [19] C. Gross and I. Bloch, Quantum simulations with ultracold atoms in optical lattices, *Science* **357**, 995 (2017).
- [20] M. Gring, M. Kuhnert, T. Langen, T. Kitagawa, B. Rauer, M. Schreitl, I. Mazets, D. A. Smith, E. Demler, and J. Schmiedmayer, Relaxation and prethermalization in an isolated quantum system, *Science* **337**, 1318 (2012).
- [21] B. Yan, S. A. Moses, B. Gadway, J. P. Covey, K. R. A. Hazzard, A. M. Rey, D. S. Jin, and J. Ye, Observation of dipolar spin-exchange interactions with lattice-confined polar molecules, *Nature* **501**, 521 (2013).
- [22] A. de Paz, A. Sharma, A. Chotia, E. Maréchal, J. H. Huckans, P. Pedri, L. Santos, O. Gorceix, L. Vernac, and B. Laburthe-Tolra, Nonequilibrium quantum magnetism in a dipolar lattice gas, *Phys. Rev. Lett.* **111**, 185305 (2013).
- [23] M. Schreiber, S. S. Hodgman, P. Bordia, H. P. Luschen, M. H. Fischer, R. Vosk, E. Altman, U. Schneider, and I. Bloch, Observation of many-body localization of interacting fermions in a quasirandom optical lattice, *Science* **349**, 842 (2015).
- [24] H. Bernien, S. Schwartz, A. Keesling, H. Levine, A. Omran, H. Pichler, S. Choi, A. S. Zibrov, M. Endres, M. Greiner, V. Vuletić, and M. D. Lukin, Probing many-body dynamics on a 51-atom quantum simulator, *Nature* **551**, 579 (2017).
- [25] A. Keesling, A. Omran, H. Levine, H. Bernien, H. Pichler, S. Choi, R. Samajdar, S. Schwartz, P. Silvi, S. Sachdev, P. Zoller, M. Endres, M. Greiner, V. Vuletić, and M. D. Lukin, Quantum kibble-zurek mechanism and critical dynamics on a programmable rydberg simulator, *Nature* **568**, 207 (2019).
- [26] P. Jurcevic, B. P. Lanyon, P. Hauke, C. Hempel, P. Zoller, R. Blatt, and C. F. Roos, Quasiparticle engineering and entanglement propagation in a quantum many-body system, *Nature* **511**, 202 (2014).
- [27] P. Richerme, Z.-X. Gong, A. Lee, C. Senko, J. Smith, M. Foss-Feig, S. Michalakakis, A. V. Gorshkov, and C. Monroe, Non-local propagation of correlations in quantum systems with long-range interactions, *Nature* **511**, 198 (2014).
- [28] J. G. Bohnet, B. C. Sawyer, J. W. Britton, M. L. Wall, A. M. Rey, M. Foss-Feig, and J. J. Bollinger, Quantum spin dynamics and entanglement generation with hundreds of trapped ions, *Science* **352**, 1297 (2016).
- [29] J. Smith, A. Lee, P. Richerme, B. Neyenhuis, P. W. Hess, P. Hauke, M. Heyl, D. A. Huse, and C. Monroe, Many-body localization in a quantum simulator with programmable random disorder, *Nature Physics* **12**, 907 (2016).
- [30] E. A. Martinez, C. A. Muschik, P. Schindler, D. Nigg, A. Erhard, M. Heyl, P. Hauke, M. Dalmonte, T. Monz, P. Zoller, and R. Blatt, Real-time dynamics of lattice gauge theories with a few-qubit quantum computer, *Nature* **534**, 516 (2016).
- [31] B. Neyenhuis, J. Zhang, P. W. Hess, J. Smith, A. C. Lee, P. Richerme, Z.-X. Gong, A. V. Gorshkov, and C. Monroe, Observation of prethermalization in long-range interacting spin chains, *Science Advances* **3**, e1700672 (2017).
- [32] P. Jurcevic, H. Shen, P. Hauke, C. Maier, T. Brydges, C. Hempel, B. P. Lanyon, M. Heyl, R. Blatt, and C. F. Roos, Direct observation of dynamical quantum phase transitions in an interacting many-body system, *Phys. Rev. Lett.* **119**, 080501 (2017).
- [33] C. Monroe, W. C. Campbell, L.-M. Duan, Z.-X. Gong, A. V. Gorshkov, P. W. Hess, R. Islam, K. Kim, N. M. Linke, G. Pagano, P. Richerme, C. Senko, and N. Y. Yao, Programmable quantum simulations of spin systems with trapped ions, *Rev. Mod. Phys.* **93**, 025001 (2021).
- [34] S. Sachdev, *Quantum Phase Transitions* (Cambridge University Press, 2009).
- [35] A. Dutta, G. Aeppli, B. K. Chakrabarti, U. Divakaran, T. F. Rosenbaum, and D. Sen, *Quantum Phase Transitions in Transverse Field Spin Models* (Cambridge University Press, 2015).
- [36] B. Damski, The simplest quantum model supporting the kibble-zurek mechanism of topological defect production: Landau-zener transitions from a new perspective, *Phys. Rev. Lett.* **95**, 035701 (2005).
- [37] W. H. Zurek, U. Dorner, and P. Zoller, Dynamics of a quantum phase transition, *Phys. Rev. Lett.* **95**, 105701 (2005).
- [38] J. Dziarmaga, Dynamics of a quantum phase transition: Exact solution of the quantum ising model, *Phys. Rev. Lett.* **95**, 245701 (2005).
- [39] A. Polkovnikov, Universal adiabatic dynamics in the vicinity of a quantum critical point, *Phys. Rev. B* **72**, 161201 (2005).
- [40] J. Dziarmaga, Dynamics of a quantum phase transition and relaxation to a steady state, *Advances in Physics* **59**, 1063 (2010).
- [41] T. W. B. Kibble, Topology of Cosmic Domains and Strings, *J. Phys. A: Math. Gen.* **9**, 1387 (1976).
- [42] T. W. B. Kibble, Some implications of a cosmological phase transition, *Physics Reports* **67**, 183 (1980).
- [43] T. W. B. Kibble, Phase-transition dynamics in the lab and the universe, *Physics Today* **60**, 47 (2007).
- [44] W. H. Zurek, Cosmological Experiments in Superfluid Helium?, *Nature* **317**, 505 (1985).
- [45] W. H. Zurek, Cosmic strings in laboratory superfluids and the topological remnants of other phase transitions, *Acta Phys. Pol. B* **24**, 1301 (1993).
- [46] W. H. Zurek, Cosmological experiments in condensed matter systems, *Physics Reports* **276**, 177 (1996).
- [47] C. Pfeleiderer, Why first order quantum phase transitions are interesting, *Journal of Physics: Condensed Matter* **17**, S987 (2005).
- [48] M. Vojta, Quantum phase transitions, *Reports on Progress in Physics* **66**, 2069 (2003).
- [49] T. Świsłocki, E. Witkowska, J. Dziarmaga, and M. Matuszewski, Double universality of a quantum phase transition in spinor condensates: Modification of the kibble-zurek mechanism by a conservation law, *Phys. Rev. Lett.* **110**, 045303 (2013).
- [50] H. Panagopoulos and E. Vicari, Off-equilibrium scaling behaviors across first-order transitions, *Phys. Rev. E* **92**, 062107 (2015).
- [51] A. Pelissetto and E. Vicari, Dynamic off-equilibrium transition in systems slowly driven across thermal first-order phase transitions, *Phys. Rev. Lett.* **118**, 030602 (2017).
- [52] I. B. Coulamy, A. Saguia, and M. S. Sarandy, Dynamics of the quantum search and quench-induced first-order phase transitions, *Phys. Rev. E* **95**, 022127 (2017).

- [53] N. Liang and F. Zhong, Renormalization-group theory for cooling first-order phase transitions in potts models, *Phys. Rev. E* **95**, 032124 (2017).
- [54] K. Shimizu, T. Hirano, J. Park, Y. Kuno, and I. Ichinose, Dynamics of first-order quantum phase transitions in extended bose hubbard model: from density wave to superfluid and vice versa, *New Journal of Physics* **20**, 083006 (2018).
- [55] L.-Y. Qiu, H.-Y. Liang, Y.-B. Yang, H.-X. Yang, T. Tian, Y. Xu, and L.-M. Duan, Observation of generalized kibble-zurek mechanism across a first-order quantum phase transition in a spinor condensate, *Science Advances* **6**, eaba7292 (2020).
- [56] A. Pelissetto, D. Rossini, and E. Vicari, Dynamic finite-size scaling after a quench at quantum transitions, *Phys. Rev. E* **97**, 052148 (2018).
- [57] A. Pelissetto, D. Rossini, and E. Vicari, Scaling properties of the dynamics at first-order quantum transitions when boundary conditions favor one of the two phases, *Phys. Rev. E* **102**, 012143 (2020).
- [58] L. D. Landau, On the theory of transfer of energy at collisions II, *Phys. Z. Sowjetunion* **2**, 56 (1932).
- [59] C. Zener, Non-adiabatic crossing of energy levels, *Proceedings of the Royal Society of London. Series A* **137**, 696 (1932).
- [60] E. Stueckelberg, Theorie der unelastischen stösse zwischen atomen, *Helvetica Physica Acta* **5**, 369 (1932).
- [61] E. Majorana, Atomi orientati in campo magnetico variabile, *Il Nuovo Cimento* **9**, 43 (1932).
- [62] C.-J. Lin and O. I. Motrunich, Quasiparticle explanation of the weak-thermalization regime under quench in a nonintegrable quantum spin chain, *Phys. Rev. A* **95**, 023621 (2017).
- [63] M. Kormos, M. Collura, G. Takács, and P. Calabrese, Real-time confinement following a quantum quench to a non-integrable model, *Nature Physics* **13**, 246 (2016).
- [64] R. Verdel, F. Liu, S. Whitsitt, A. V. Gorshkov, and M. Heyl, Real-time dynamics of string breaking in quantum spin chains, *Phys. Rev. B* **102**, 014308 (2020).
- [65] P. I. Karpov, G. Y. Zhu, M. P. Heller, and M. Heyl, Spatiotemporal dynamics of particle collisions in quantum spin chains, [arXiv:2011.11624](https://arxiv.org/abs/2011.11624).
- [66] F. M. Surace and A. Lerose, Scattering of mesons in quantum simulators, [arXiv:2011.10583](https://arxiv.org/abs/2011.10583).
- [67] A. A. Michailidis, C. J. Turner, Z. Papić, D. A. Abanin, and M. Serbyn, Slow quantum thermalization and many-body revivals from mixed phase space, *Phys. Rev. X* **10**, 011055 (2020).
- [68] A. J. A. James, R. M. Konik, and N. J. Robinson, Nonthermal states arising from confinement in one and two dimensions, *Phys. Rev. Lett.* **122**, 130603 (2019).
- [69] N. J. Robinson, A. J. A. James, and R. M. Konik, Signatures of rare states and thermalization in a theory with confinement, *Phys. Rev. B* **99**, 195108 (2019).
- [70] S. Pai and M. Pretko, Fractons from confinement in one dimension, *Phys. Rev. Research* **2**, 013094 (2020).
- [71] J. Haegeman, J. I. Cirac, T. J. Osborne, I. Pizorn, H. Verschelde, and F. Verstraete, Time-dependent variational principle for quantum lattices, *Phys. Rev. Lett.* **107**, 070601 (2011).
- [72] T. Koffel, M. Lewenstein, and L. Tagliacozzo, Entanglement entropy for the long-range ising chain in a transverse field, *Phys. Rev. Lett.* **109**, 267203 (2012).
- [73] J. Haegeman, C. Lubich, I. Oseledets, B. Vandereycken, and F. Verstraete, Unifying time evolution and optimization with matrix product states, *Phys. Rev. B* **94**, 165116 (2016).
- [74] J. R. Schrieffer and P. A. Wolff, Relation between the anderson and kondo hamiltonians, *Phys. Rev.* **149**, 491 (1966).
- [75] See supplementary material for details.
- [76] A. V. Shytov, Landau-zener transitions in a multilevel system: An exact result, *Phys. Rev. A* **70**, 052708 (2004).
- [77] S. Ebadi, T. T. Wang, H. Levine, A. Keesling, G. Semeghini, A. Omran, D. Bluvstein, R. Samajdar, H. Pichler, W. W. Ho, S. Choi, S. Sachdev, M. Greiner, V. Vuletic, and M. D. Lukin, Quantum phases of matter on a 256-atom programmable quantum simulator, [arXiv:2012.12281](https://arxiv.org/abs/2012.12281).
- [78] P. Scholl, M. Schuler, H. J. Williams, A. A. Eberharter, D. Barredo, K.-N. Schymik, V. Lienhard, L.-P. Henry, T. C. Lang, T. Lahaye, A. M. Läuchli, and A. Browaeys, Programmable quantum simulation of 2d antiferromagnets with hundreds of rydberg atoms, [arXiv:2012.12268](https://arxiv.org/abs/2012.12268).

Supplementary material to “Non-adiabatic dynamics across a first order quantum phase transition: Quantized bubble nucleation”

Aritra Sinha,^{1,*} Titas Chanda,^{1,†} and Jacek Dziarmaga^{1,‡}

¹*Institute of Theoretical Physics, Jagiellonian University, Lojasiewicza 11, 30-348 Kraków, Poland*
(Dated: June 10, 2021)

Here we present the derivation of effective two-level Hamiltonians near the resonant points using Schrieffer-Wolff transformation and the general Landau-Zener probability for an n -bubble nucleation process. Furthermore, we present some additional details to complement the main text. Specifically, we discuss details about the multi-level Landau-Zener problem beyond the low density regime.

Effective Hamiltonian near second order resonant point

To understand the physics near the 2nd order resonant point (RP₂) at $h_z = 1$, we need to construct a simple effective Hamiltonian using the Schrieffer-Wolff transformation [1]. Following the idea of low density approximations discussed in the main text only the following *local* process is allowed near RP₂:

$$|\downarrow \dots \downarrow \downarrow_j \downarrow_{j+1} \downarrow \dots \downarrow\rangle_{|M\rangle} \xleftrightarrow{h_x^2} |\downarrow \dots \downarrow \uparrow_j \uparrow_{j+1} \downarrow \dots \downarrow\rangle_{|T_2\rangle}. \quad (1)$$

The calculation done below closely follows similar calculations done in references [2, 3]. We take $H = H^0 + V$, with

$$H^0 = - \sum_{n=1}^N [\sigma_n^z \sigma_{n+1}^z + h_z \sigma_n^z] \quad (2)$$

being the unperturbed Hamiltonian and

$$V = -h_x \sigma_n^x \quad (3)$$

as the perturbation.

We carry out a unitary transformation with generator S such that the rotated Hamiltonian has no first order term:

$$\begin{aligned} \hat{H} &= e^S H e^{-S} \\ &= H^0 + V + [S, H^0] + [S, V] + \frac{1}{2}[S, [S, H^0]] + \dots \end{aligned} \quad (4)$$

Therefore, we need to set $[S, H^0] = -V$ to get rid of first order perturbation, and in the basis of the unperturbed Hamiltonian H^0 , we get

$$S_{ij} = V_{ij}/(\epsilon_i - \epsilon_j) \quad (5)$$

where $V_{ij} = \langle i|V|j\rangle$, providing us our rotated Hamiltonian

$$\hat{H} = H^0 + \frac{1}{2}[S, V] \quad (6)$$

up to second order in perturbation.

Now, we need to identify the shortest paths which connect the states $|M\rangle$ and $|T_2\rangle$. This takes place

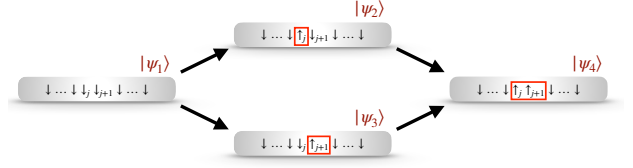


FIG. 1. The sketch illustrates the the Ising states relevant in the process connecting the meta-stable state $|\psi_1\rangle$ to the target 2-bubble nucleated state $|\psi_4\rangle$ under the effective second order (in perturbation) Hamiltonian H_{eff}^2 . Each dark arrow connects two Ising states by an order of perturbation h_x .

through the states $|C_1\rangle = |\downarrow \dots \downarrow \uparrow_j \downarrow_{j+1} \downarrow \dots \downarrow\rangle$ and $|C_2\rangle = |\downarrow \dots \downarrow \downarrow_j \uparrow_{j+1} \downarrow \dots \downarrow\rangle$. Thereafter we construct the relevant subspace using the four states (see Fig. 1 for the processes involving the states in the subspace):

$$|\psi_1\rangle = |M\rangle; |\psi_2\rangle = |C_1\rangle; |\psi_3\rangle = |C_2\rangle; |\psi_4\rangle = |T\rangle.$$

In this subspace, we have the unperturbed Hamiltonian H^0 as a 4×4 diagonal matrix containing the non-zero elements: $H_{ii}^0 = \langle \psi_i | H^0 | \psi_i \rangle$. Similarly from (3) and (5), we get

$$V = -h_x \begin{bmatrix} 0 & 1 & 1 & 0 \\ 1 & 0 & 0 & 1 \\ 1 & 0 & 0 & 1 \\ 0 & 1 & 1 & 0 \end{bmatrix} \quad \text{and} \quad S = \begin{bmatrix} 0 & a & a & 0 \\ -a & 0 & 0 & b \\ -a & 0 & 0 & b \\ 0 & -b & -b & 0 \end{bmatrix} \quad (7)$$

where $a = \frac{h_x}{2h_z - 4}$ and $b = -\frac{h_x}{2h_z}$.

Now if we take into account only the basis spanned by the initial meta-stable state ($|\psi_1\rangle$) and the target resonant state ($|\psi_4\rangle$), we get an effective two-level system as desired for Landau Zener probability calculations:

$$H_{\text{eff}}^{(2)} = \begin{bmatrix} H_{11}^0 - \frac{h_x^2}{2-h_z} & -\frac{h_x^2}{2h_z - h_z^2} \\ -\frac{h_x^2}{2h_z - h_z^2} & H_{44}^0 - \frac{h_x^2}{h_z} \end{bmatrix}$$

where $H_{11}^0 = -(N-1) + Nh_z$ and $H_{44}^0 = -(N-5) + (N-4)h_z$. Near RP₂ at $h_z = 1$, the off-diagonal terms reduce to just $-h_x^2$; while in the limit $h_x \ll 1$, the h_x^2 contribution in the diagonal terms can be neglected. The final form is

$$H_{\text{eff}}^{(2)} \approx E_0(h_z) + \begin{bmatrix} 0 & -h_x^2 \\ -h_x^2 & 4 - 4h_z \end{bmatrix}. \quad (8)$$

Here $E_0(h_z) = H_{11}^0 = -(N-1) + Nh_z$ is energy of the meta-stable state.

Effective Hamiltonian near third order resonant point

The processes allowed near the 3rd resonant point (RP₃) at $h_z = 2/3$ involve a 3-bubble nucleation as the following:

$$|\downarrow \dots \downarrow \downarrow_j \downarrow_{j+1} \downarrow_{j+2} \dots \downarrow\rangle_{|M\rangle} \xleftrightarrow{h_x^3} |\downarrow \dots \downarrow \uparrow_j \uparrow_{j+1} \uparrow_{j+2} \dots \downarrow\rangle_{|T_3\rangle}, \quad (9)$$

Here too we transform the Hamiltonian through a generator S , to get rid of the first order and second order terms and put into prominence the third order perturbation which governs the low energy physics near RP₃. To do that we expand $S = S_1 + S_2$ as a sum of two terms. Here $S_1 \sim \mathcal{O}(h_x)$ kills the first order terms of the transformed Hamiltonian and $S_2 \sim \mathcal{O}(h_x^2)$ gets rid of the second order terms. The transformation applied on the Hamiltonian goes like $\hat{H} = e^{S_2} e^{S_1} H e^{-S_1} e^{-S_2}$. As before we collect the first order and second order terms and set them to 0 to obtain two conditions in order to determine the explicit forms of S_1 and S_2 :

$$\begin{aligned} [S_1, H_0] &= -V, \\ [S_2, H_0] &= -\frac{1}{2}[S_1, V]. \end{aligned} \quad (10)$$

Using (10), the transformed Hamiltonian upto 3rd order in perturbation looks like :

$$\hat{H} = H_0 + [S_2, V] + \frac{1}{2}[S_1 H_0 S_1, S_1] + \frac{1}{6}[S_1^3, H_0]. \quad (11)$$

Having done the mathematical analysis, we need to construct the basis which connects $|M\rangle$ to $|T_3\rangle$. See the sketch in Fig. 2 as an aid to visualize the perturbative processes involved among the states in the subspace, and also for the labels of states considered in the following discussion. There are a minimum 8 unique basis states in such a process: $\{|\psi_i\rangle; i = 1, \dots, 8\}$ with $|\psi_1\rangle = |M\rangle$ and $|\psi_8\rangle = |T_3\rangle$. After performing calculations with the basis states, we arrive at an effective two-level form of the rotated Hamiltonian in (11) connecting $|\psi_1\rangle$ and $|\psi_8\rangle$ through a third order process at $h_z = 2/3$:

$$H_{\text{eff}}^{(3)} \approx E_0(h_z) + \begin{bmatrix} 0 & -\frac{81}{64}h_x^3 \\ -\frac{81}{64}h_x^3 & 4 - 6h_z \end{bmatrix}. \quad (12)$$

Landau Zener Calculations

In this section of the supplementary text, we calculate the Landau Zener probability to nucleate a bubble of

size n near $h_z = 2/n$, from an initial metastable state. To do this we apply the Landau-Zener formula [4-7] after transforming the effective two-level problem to an appropriate framework.

Consider flipping n consecutive spins $j, \dots, j+n-1$ by a n -th order process:

$$|\downarrow \dots \downarrow \downarrow_j \dots \downarrow_{j+n-1} \downarrow \dots \downarrow\rangle_{|A\rangle} \xleftrightarrow{h_x^n} |\downarrow \dots \downarrow \uparrow_j \dots \uparrow_{j+n-1} \downarrow \dots \downarrow\rangle_{|B\rangle}. \quad (13)$$

For such a process the general effective Hamiltonian reads

$$H_{\text{eff}}^{(n)} \approx E_0(h_z) + \begin{bmatrix} 0 & -c_n h_x^n \\ -c_n h_x^n & 4 - 2nh_z \end{bmatrix}. \quad (14)$$

where c_n is a constant for a specific perturbative process. Comparing with effective Hamiltonians (8) and (12) in the previous sub-sections, it is $c_2 = 1$ for a second order and $c_3 = 81/64$ for third-order process.

Rescaling the energy of effective Hamiltonian for such processes (see (14)), we arrive at

$$H_{\text{eff}}^{(n)} \approx \begin{bmatrix} -2 + nh_z & -c_n h_x^n \\ -c_n h_x^n & 2 - nh_z \end{bmatrix}.$$

Let us linearize the longitudinal field as

$$h_z = t/\tau_Q + 2/n \quad (15)$$

where t goes from $-\infty$ to ∞ such that at $t = 0$ the ramp is centered on the resonant point at $h_z = 2/n$. If

$$|\psi(t)\rangle = \alpha(t)|A\rangle + \beta(t)|B\rangle \quad (16)$$

then the Schrodinger equation $i \frac{d}{dt} |\psi\rangle = H_{\text{eff}}^{(n)} |\psi\rangle$ for $\alpha(t)$ and $\beta(t)$ is given by a set of coupled differential equations:

$$i \frac{d}{dt} \begin{pmatrix} \alpha \\ \beta \end{pmatrix} = \begin{bmatrix} nt/\tau_Q \sigma^z - c_n h_x^n \sigma^x \\ \tau_Q \sigma^z - c_n h_x^n \sigma^x \end{bmatrix} \begin{pmatrix} \alpha \\ \beta \end{pmatrix} \quad (17)$$

Defining $t' = -nth_x$ and $\Delta = (2 \frac{c_n}{n} \tau_Q h_x^{2n})^{-1}$ we get

$$i \frac{d}{dt'} \begin{pmatrix} \alpha \\ \beta \end{pmatrix} = \frac{1}{2} [\Delta t' \sigma^z + \sigma^x] \begin{pmatrix} \alpha \\ \beta \end{pmatrix} \quad (18)$$

Say we initialize the system in state $|A\rangle$. The initial condition is then given by $\alpha(t = -\infty) = 1$, $\beta(t = -\infty) = 0$. Here we are interested in the occupation probabilities of the states at $t \rightarrow +\infty$. Note that after the anti-crossing ($t > 0$) the metastable state $|A\rangle$ is the excited state and if the transition in the parent model was fully adiabatic the probability to stay in $|B\rangle$ at $t \rightarrow +\infty$ would be 1. With this consideration, the probability for the system to remain in $|B\rangle$ or in the present context, the probability that a spin flip of size n occurs at the chosen site in $|B\rangle$ is given by $|\beta(t = \infty)|^2 = 1 - \exp(-\pi/2\Delta) \approx \pi/2\Delta = \frac{c_n}{n} \pi \tau_Q h_x^{2n}$ assuming $\tau_Q h_x^{2n} \ll 1$ for physical reasons elaborated in the main text.

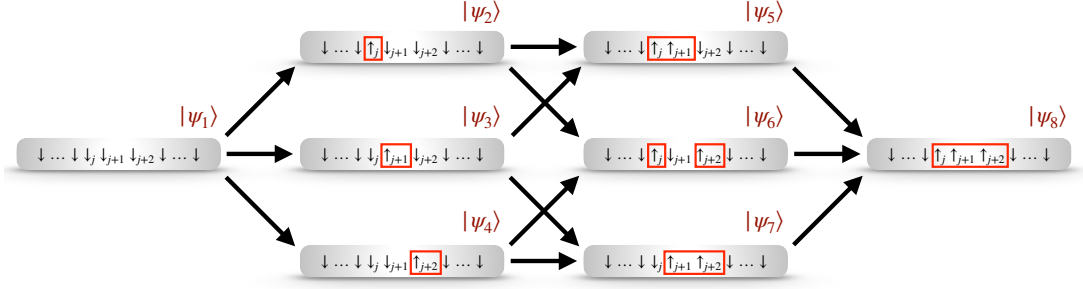


FIG. 2. The sketch illustrates the the Ising states relevant in the process connecting the meta-stable state $|\psi_1\rangle$ to the target 3-bubble nucleated state $|\psi_8\rangle$ under the effective 3rd order (in perturbation) Hamiltonian H_{eff}^3 . Each dark arrow connects two Ising states by an order of perturbation h_x .

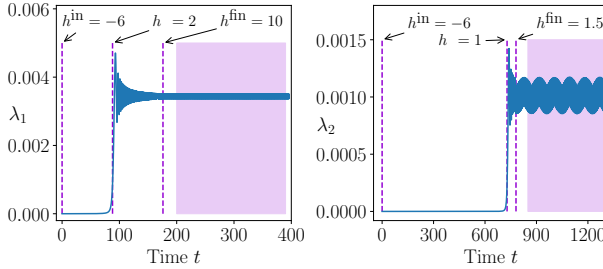


FIG. 3. (Left) Density profile of 1-bubbles λ_1 versus time for a fixed transverse field strength $h_x = 0.01$ for $\tau_Q = 11$. (Right) Profile of the 2-bubble density λ_2 with time for transverse field strength $h_x = 0.05$ with $\tau_Q = 104$. In both the cases, we stop the ramp at h_z^{fin} and then perform free evolution with fixed h_z^{fin} . The averaging is performed over the oscillations in the region shaded with violet.

Calculation of the observables

To verify the predictions offered by Landau-Zener theory we calculate the n -bubble density (Eq.(10) in the main text). In that respect, we follow the quench protocol of Eq. (2) of the main text upto $h_z = h_z^{\text{fin}}$, then proceed with free evolution with the fixed longitudinal field h_z^{fin} for a long time. In the case of 1-bubbles, the ramp is simulated from $h_z^{\text{in}} = -6$ to $h_z^{\text{fin}} = 10$, while for 2-bubbles we set h_z^{in} to be 1.5, and for 3-bubbles $h_z^{\text{fin}} = 0.8$. In order to get n -bubble density λ_n ($n = 1, 2, 3$), we average generously over the oscillations during the free evolution. See Fig. 3 for sample time profiles for the observables λ_1 and λ_2 during the ramp. We denote the h_z^{in} and h_z^{fin} , i.e., the start and end-points of the ramp by dashed vertical lines and the violet shaded region demarcates the region of the oscillatory part we average over.

Beyond the low density regime: details

To look at the 1-bubble nucleation in full isolation, we project our original Hamiltonian (Eq. (1) in the main text) onto a 1-bubbles subspace. We start with the initial metastable state $|0\rangle = |\psi_{\text{in}}\rangle$ (Eq. (3) in the main text), and generate states with increasing number of 1-bubbles iteratively from that. For example, single spin flips on $|0\rangle$ will create the translationally invariant (TI) one 1-bubble state

$$|1\rangle = \frac{1}{\sqrt{N}} \sum_j |\downarrow \dots \downarrow \uparrow_j \downarrow \dots \downarrow\rangle, \quad (19)$$

another set of single spin flips on $|1\rangle$ generates the TI two 1-bubble state

$$|2\rangle = \frac{1}{\sqrt{N(N-1)}} \sum_{\substack{j_1, j_2 \\ j_2 \neq j_1 \pm 1}} |\downarrow \dots \downarrow \uparrow_{j_1} \downarrow \dots \downarrow \uparrow_{j_2} \downarrow \dots \downarrow\rangle, \quad (20)$$

upto the TI $N/2$ 1-bubble state.

$$|N/2\rangle = \frac{1}{\sqrt{2}} (|\downarrow \uparrow \downarrow \uparrow \dots\rangle + |\uparrow \downarrow \uparrow \downarrow \dots\rangle) \quad (21)$$

Moreover, in this scheme, the n 1-bubble state can be constructed iteratively from $(n-1)$ 1-bubble state by applying $\sum_j \sigma_j^+$ on the state $|n-1\rangle$ with the condition that no neighboring spins can be \uparrow -spin, i.e.,

$$|n-1\rangle \xrightarrow{\sum_j \sigma_j^+ \text{ with the condition}} \frac{D_n}{\sqrt{F_{n-1} F_n}} |n\rangle, \quad (22)$$

where D_n and F_n s are combinatorial integers. The projected Hamiltonian in the basis $\{|n\rangle, n = 0, 1, \dots, N/2\}$ has the following tri-diagonal form

$$\begin{aligned} (H_{\text{eff}})_{(n,n)} &= 2n(2 - h_z) + E_0(h_z), \\ (H_{\text{eff}})_{(n,n-1)} &= (H_{\text{eff}})_{(n-1,n)} = -h_x \frac{D_n}{\sqrt{F_{n-1} F_n}}. \end{aligned} \quad (23)$$

Therefore, following the convention of Eq. (12) in the main text, we get

$$(H_z)_{(n,n)} = -2n, \\ (H_x)_{(n,n-1)} = (H_x)_{(n-1,n)} = -\frac{D_n}{\sqrt{F_{n-1}F_n}}. \quad (24)$$

To get the transition probability $p_{0 \rightarrow 0}$ (see Eq. (14) of the main text), only relevant terms are $(H_x)_{(1,0)}$ and $(H_z)_{(0,0)}$. Moreover, it is easy to check that $(H_x)_{(1,0)} = (H_x)_{(0,1)} = \sqrt{N}$, giving us the closed analytical form $p_{0 \rightarrow 0} = \exp[-N\pi\tau_Q h_x^2]$.

Finding the closed analytical form of the transition probability $p_{0 \rightarrow \frac{N}{2}}$ is beyond the scope of our work, and we resort to numerical results. As already mentioned in the main text, we find that

$$p_{0 \rightarrow \frac{N}{2}} = 1 - \exp[-\alpha_N \pi \tau_Q h_x^2], \quad (25)$$

with the coefficient α_N being dependant on the system size N . Below, we tabulate the numerical values of α_N found for different system-sizes:

System size N	14	20	26	32	38	44
Coefficient α_N	0.36	0.27	0.22	0.19	0.16	0.14

Here the errors in the fitting are below 10^{-4} .

* aritrashin98@gmail.com

† titas.chanda@uj.edu.pl

‡ dziarmaga@th.if.uj.edu.pl

- [1] J. R. Schrieffer and P. A. Wolff, Relation between the anderson and kondo hamiltonians, *Phys. Rev.* **149**, 491 (1966).
- [2] C.-J. Lin and O. I. Motrunich, Quasiparticle explanation of the weak-thermalization regime under quench in a nonintegrable quantum spin chain, *Phys. Rev. A* **95**, 023621 (2017).
- [3] R. Verdel, F. Liu, S. Whitsitt, A. V. Gorshkov, and M. Heyl, Real-time dynamics of string breaking in quantum spin chains, *Phys. Rev. B* **102**, 014308 (2020).
- [4] L. D. Landau, On the theory of transfer of energy at collisions II, *Phys. Z. Sowjetunion* **2**, 56 (1932).
- [5] C. Zener, Non-adiabatic crossing of energy levels, *Proceedings of the Royal Society of London. Series A* **137**, 696 (1932).
- [6] E. Stueckelberg, Theorie der unelastischen stösse zwischen atomen, *Helvetica Physica Acta* **5**, 369 (1932).
- [7] E. Majorana, Atomi orientati in campo magnetico variabile, *Il Nuovo Cimento* **9**, 43 (1932).